X-ray scattering of non-crystalline biological systems using synchrotron radiation

Michel H. J. Koch

Received 18th August 2005
First published as an Advance Article on the web 21st November 2005
DOI: 10.1039/b500858c

This *tutorial review* gives an overview of the progress in the study of non-crystalline systems by X-ray scattering and closely related imaging techniques, made possible by advances in synchrotron radiation sources and instrumentation. A brief introduction to the techniques is followed by the presentation of a variety of recent applications to problems in fundamental and applied research in biochemistry and biophysics and food and pharmaceutical technology.

1 Introduction

Several new synchrotron radiation (SR) and neutron sources have recently been built or are under construction worldwide in the wake of the current interest in the organisation of matter on the nano- and mesoscopic scale. This has also resulted in renewed attention to X-ray and neutron scattering which are among the few well established non-destructive methods for studying the structure of non-crystalline matter at length scales of a few Ångstroms to a few hundred nm. These techniques thus bridge the gap in spatial resolution between electron microscopy and atomic force microscopy, which are limited to small samples, and diffraction methods which require crystals. SR sources also make time resolved measurements possible—even with small samples (<100 μm)—on time scales that are relevant to the processing of materials.

Although the present review emphasizes recent applications of SR X-ray scattering, and closely related imaging techniques in the life sciences it should be borne in mind that scattering studies on synthetic polymers, colloids or inorganic systems represent a much broader field of application. There are also many interesting applications of SR to the study of non-crystalline biological systems in the infrared and UV range.

The superiority of SR sources over conventional ones for scattering and imaging lies in their much higher spectral brilliance (*i.e.* number of photons emitted per unit area of the source, unit solid angle, 0.1% bandpass and unit time). Combined with the continuous energy tunability of these sources, the high spectral brilliance, which implies a small source size, a small beam divergence and a high beam flux, has very much improved the conditions for scattering experiments. On the most modern sources the partial coherence of the radiation also offers new possibilities for direct imaging.

For many applications where time resolution or wavelength tunability are not indispensable an optimized conventional instrument[1] certainly still offers an attractive and cost effective alternative to the travel and delays often associated with the use of large facilities.

European Molecular Biology Laboratory, Hamburg Outstation, EMBL c/o DESY, Notkestrasse 85, D-22603 Hamburg, Germany. E-mail: koch@embl-hamburg.de; Fax: +494089902149; Tel: +494089902113

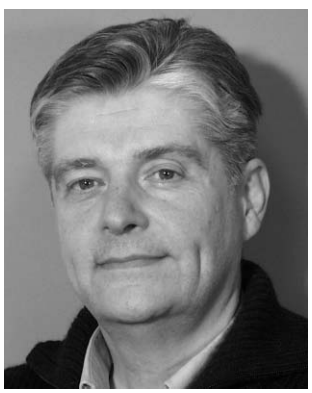

Michel H. J. Koch

Michel Koch studied chemistry and biology at the Catholic University of Louvain where he obtained a PhD in 1970. In the following years he worked as a postdoctoral fellow in the Physics Department of the University of York and as a consultant for Janssen Pharmaceutica and collaborated with H. B. Stuhrmann in neutron scattering studies of biological systems. Since 1977 he has served in different functions at the outstation of the European Molecular Biology Laboratory at the Deutsches Elektronen Synchrotron (DESY) in Hamburg. His research interests have centered around the study of structural changes in biological and synthetic systems.

2 Developments

Biological materials come in different forms including solutions, gels and liquid crystalline assemblies, fibres, membranes and vesicles reflecting the important role of intermolecular forces in these very smart materials based on millions of years of evolution. No wonder thus that chemists with their few thousand years of experience would not yet be able to match these achievements. To cope with this variety a number of different but complementary experimental and theoretical approaches were developed during the last century.

The basic principles of small angle X-ray scattering (SAXS) by non-crystalline materials (see *e.g.*[2]) were already well understood in the 1930s through the work of Guinier[3] and others. Because of the low brilliance of the available X-ray sources applications to biological systems remained the work of a few pioneers. Further progress in small angle scattering on monodisperse solutions of biological macromolecules came from the introduction of the formalism of contrast variation and of spherical harmonics for the interpretation of scattering patterns in the early 1970s (see[4] and references therein).

At about the same time fibre diffraction and in particular the study of muscle contraction using whole frog or insect muscle provided the initial driving force for using SR for biophysical applications.[5] The theory of fibre diffraction also took longer to develop than that of small angle scattering and was only published in the 1950s.[6]

Many biological macromolecules such as DNA, RNA and components of the cytoskeleton like actin, collagen, intermediate filaments, keratin and silk, naturally or artificially form fibres with helical symmetry. The polycrystalline fibres consist of elongated microcrystals randomly oriented around the common fibre axis giving rise to a diffraction pattern with reflections arranged on equally spaced layer lines as defined by the periodicity along the fibre axis. In the non-crystalline fibres the individual molecules still have their long axis parallel to the fibre axis but they are otherwise randomly oriented which gives rise to a continuous intensity distribution along the layer lines. Compared to standard crystallography, interpretation of fibre diffraction patterns (see *e.g.*[2]) remains an art even though considerable progress has been made.[7]

Interpretation of the scattering patterns of lipid–water systems, including those containing proteins and/or nucleic acids, and membranes also remains a challenge. Although such systems usually scatter well, their X-ray patterns, which contain only a handful of reflections, are difficult to interpret without additional information. To complicate matters these systems display a rich polymorphism.[8] The study of their static and dynamic phase diagrams requires a large number of measurements which are most easily carried out on SR sources. The results from some of these studies on bulk systems have an impact in various realms ranging from physiology to pharmaceutical technology and catalysis. SR has, however, also made more systematic investigations of the structure of monolayers and membranes using grazing incidence X-ray scattering feasible and these have produced many interesting results.[9]

The advances in SR sources, optics, detectors and data interpretation methods between 1980 and 2000 led to more applications of time resolved scattering and diffraction than had previously been possible on conventional sources. This is particularly true in the fields of biophysics, synthetic polymers and colloidal systems. Although several more recent areas of progress, such as X-ray microscopy (see[10] and references therein), refractive optics,[11] the use of coherent radiation[12] and phase contrast imaging,[13] which are more than mere extensions of previous work with higher fluxes, can be expected to acquire a growing importance in the study of non-crystalline materials, including biological samples, they cannot be covered in any detail here.

3 Basic principles

The basic layout of an X-ray scattering instrument is illustrated in Fig. 1. It consists of a source, a mirror and a monochromator, a collimation system, a sample cell and a detector and data acquisition system. A real instrument is, of course, somewhat more complicated as illustrated by the plans for the new SAXS station at the Diamond Light Source.[14]

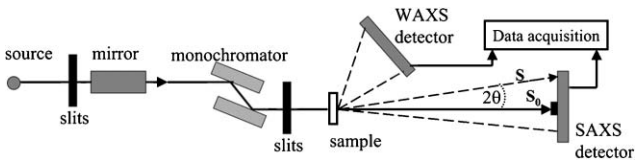

Fig. 1 Schematic representation of a small and wide angle X-ray scattering (SWAXS) camera. For a scattering angle 2θ and an X-ray wavelength λ the modulus of the scattering vector, corresponding to a spatial resolution d is $s = 1/d = 2\sin\theta/\lambda$. The literature often refers to the corresponding momentum transfer: $q = S = h = 4\pi\sin\theta/\lambda$.

When X-rays interact with matter the electromagnetic field of the incident plane wave accelerates the individual electrons in the sample, which oscillate and become the source of spherical waves. These interfere giving rise to the scattering pattern which is recorded as a function of the scattering vector $\boldsymbol{s} = \boldsymbol{S}/\lambda - \boldsymbol{S}_0/\lambda$ or, for isotropic systems like powders, solutions or gels, as a function of its modulus ($|\boldsymbol{s}| = s = 2\sin\theta/\lambda$), or of the scattering angle 2θ between the directions of propagation of the incident ($\boldsymbol{S}_0$) and scattered ($\boldsymbol{S}$) waves. Whereas for small angle scattering polarisation effects are negligible, as they are a function of $\cos 2\theta$ depending on the exact geometry of the measurement, this is not the case for wide angle scattering where appropriate corrections must be made.

In coherent elastic scattering the energy (or wavelength λ) is conserved and the scattered waves, which are in antiphase with the incident wave, interfere in a manner defined by the positions and nature of the scattering atoms. Indeed, the contribution of each pair of atoms to the scattered intensity for a given scattering vector is determined by their atomic scattering factors ($f(s)$), which are independent of the wavelength, and by a phase factor $\cos[2\pi(\boldsymbol{s}\cdot\boldsymbol{r}_{ij})]$, depending solely on their distance ($\boldsymbol{r}_{ij}$). In Cartesian coordinates the intensity is given by eqn 1.

$$I(\boldsymbol{s}) = \sum_{i=1}^{N}\sum_{j=1}^{N} f_i f_j \cos\left[2\pi\left(\boldsymbol{s}\cdot\boldsymbol{r}_{ij}\right)\right] \qquad (1)$$

Close to absorption edges of specific (heavy) elements corrections depending on λ must be made to the scattering factors to take anomalous dispersion into account. The complete expression for the scattering factor is then ($f(s,\lambda) = f(s) + f'(\lambda) + if''(\lambda)$) where the imaginary correction f'' describes the fact that the incident and scattered waves are no longer exactly in antiphase. The imaginary correction f'' is directly related to the linear absorption coefficient (μ), the quantity measured in X-ray absorption spectroscopy (XAS), and is linked to the value of f' by the Kramers–Kronig relationship.

A large fraction of the incident intensity gives rise to inelastic (Compton), incoherent scattering. In this case the scattered waves have a lower energy than the incident one and there is no fixed relationship between their phases. Consequently, no interferences occur and this type of scattering therefore does not contain any structural information but contributes to the background. With dilute solutions the background is usually easily eliminated together with that of other sources such as windows, slits *etc.*, by subtracting the

scattering of the solvent measured in identical conditions. For solid samples (*e.g.* starch) interpretation is more complicated and a number of assumptions, such as the existence of a two-phase system, must usually be made.

It is implicit in the above discussion that the incident wave must be coherent over dimensions larger than those of the fluctuations in electron density which one wishes to observe. For a quasi-monochromatic incoherent source with wavelength λ the coherence length in the direction of propagation of the wave or longitudinal coherence length ($\Lambda \sim \lambda^2/\Delta\lambda$) corresponds effectively to the distance over which two waves with a wavelength difference of $\Delta\lambda$ become out of phase. Λ is determined by the bandpass, $\Delta\lambda/\lambda$ of the monochromator[15] and for a typical crystal monochromator with a bandpass of $\Delta\lambda/\lambda = 10^{-4}$ its value is about 0.5 μm. In contrast, the area of the sample which is coherently illuminated, or transverse coherence area (S), depends on the source size (a) and the distance (R) between the source and the sample ($S \sim \lambda^2 R^2/a$). On conventional sources or second generation SR sources the transverse coherence area is small (<1 μm^2), but on newer sources the small source dimensions and large source–sample distances (>50 m) result in values of the order of several hundred μm^2, which offers new possibilities for imaging.

Ideally one would of course like to image structures directly and various approaches can be used as illustrated in Fig. 2 but as the value of the refractive index of all materials for hard X-rays is very close to unity the possibilities of making lenses are severely limited. Indeed, the maximum spatial resolution which can be obtained with a lens of refractive index n is limited by its numerical aperture (NA) to $\sim 0.61\ \lambda/\mathrm{NA}$, where $\mathrm{NA} = n \sin\varphi$ and φ is half the angle of the image forming cone. Estimates for the upper limit of spatial resolution achievable with X-ray lenses presently range between 20 and 2 nm, suggesting that there still is a significant margin for improvement.[11]

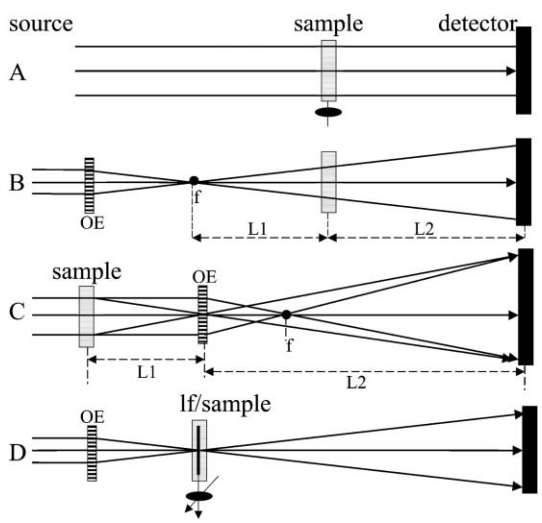

Fig. 2 Schematic representation of different types of X-ray microscopes, with maximum resolutions ranging between a few μm and 30 nm (after[10]). Kirkpatrick–Baez mirrors, Fresnel zone plates or refractive lenses are used as optical element (OE). A: simple projection, a 3D picture can be obtained by rotating the sample and combining the projections (tomography); B: with $L2 \gg L1$ a magnified phase contrast image is obtained on the detector; C: In a standard microscope the sample placed at a distance L1 slightly larger than the focal distance f is illuminated by a quasi-monochromatic beam and yields an image with a magnification $L2/L1$. D: scanning microscope where the sample is translated across a line shaped beam to obtain a magnified projection and rotated for tomography.

If the transverse coherence is sufficiently large, the small deviations of the refractive index for hard X-rays from unity, ($n = 1 - \delta + i\beta$) can be put to good use for phase contrast imaging. The absorptive increment $\beta = \lambda\ \mu/4\pi$, is proportional to the linear absorption coefficient μ and thus to f'', whereas the dispersive decrement δ is proportional to the electron density and thus to the real part of the scattering factor. At low energies β is larger than δ and a (radiographic) transmission image is obtained which depends on absorption contrast and where coherence does not matter.

As the value of the mass absorption coefficient (μ/ρ, where ρ is the density) of an element with atomic number Z decreases as $(Z/E)^3$ between absorption edges, at energies (E) between 15–25 keV ($\lambda \approx 0.5$–0.8 Å) organic material becomes effectively transparent (*i.e.* $n = 1 - \delta$ with $\delta \sim 10^{-6}$). This implies that the X-rays are deflected by a few microradians, which is, of course, considerably less than the angles associated with scattering (*i.e.* a few milliradians). If the detector is placed close to the sample a simple transmission image is obtained, but at larger sample–detector distances (~ 1 m) the X-rays have travelled sufficiently far for the interference effects due to the phase shift resulting from the path length difference between different rays to become detectable. Contrast is enhanced especially in the vicinity of edges separating regions of different electron densities. These effects can be understood in terms of Fresnel or near field diffraction[13] and methods are being developed to recover the phase information. One way of separating the contributions of scattering, absorption and refraction is to use a Bonse–Hart or ultra small angle scattering (USAXS) camera,[16] where the sample is placed between a monochromator and an analyser crystal, as illustrated in Fig. 3. Although in scattering experiments these devices provide resolutions in the μm-range on bulk samples their obvious limitation is that the analyser crystal must be scanned and that the scattering patterns can only be recorded point by point. Applications to biological samples have therefore hitherto been limited to the study of large structures like striated muscle, where the technique has been used to prove the existence of large transverse periodicities.[17] Imaging applications could considerably extend the range of application of these instruments. Indeed, as the analyser crystal only

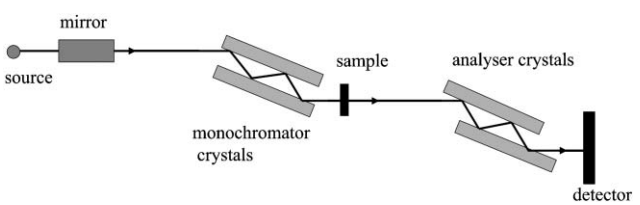

Fig. 3 Schematic representation of an Ultra Small Angle Scattering (USAXS) or Bonse–Hart camera. The small angle resolution of these devices, which can be used for scattering or imaging, overlaps with that of optical microscopy.

reflects rays with incident angles falling within the small angular range defined by its rocking curve (usually $\pm$ 5 μrad), it filters out most of the scattering. By detuning the crystal and recording images on both sides of the rocking curve it also becomes possible to separate the contribution of refraction and absorption. The direct recovery of phase information from scattering or refraction patterns is a very active area of research where spectacular progress is being made.

4 Data collection

In X-ray scattering the exact choice of s-range, wavelength and sample size depends on the particular experiment, sample, instrument and detector. In particular, the choice of wavelength, which depends on absorption and detector efficiency, must also take into account the fact that the Compton/coherent elastic scattering ratio decreases at higher energy.

The higher brightness of modern sources has inevitably exacerbated the difficulties associated with radiation and even heat damage. The standard ways of minimizing these effects are cooling, addition of free radical scavengers and displacing or flowing the sample. In any case, it is good practice to attenuate the beam to the minimum level required for a particular experiment.

Sample environments and devices, ranging from the very simple to the very sophisticated reflecting the variety of experiments which can be done with X-ray scattering have been described in the literature.

Static scattering measurements on solutions of biological macromolecules which can have volumes as small as a few μl with concentrations of 1–10 mg ml^{-1} on modern instruments, are usually contained in thermostated cells with mica windows or in capillaries. Measurement of wide-angle X-ray scattering (WAXS) patterns requires solutions with high protein concentrations (>10 mg ml^{-1}) and great care must be taken to avoid artefacts due to background subtraction.[18] Depending on the experimental geometry it may also be necessary to apply polarisation corrections.

During the last decades most perturbation techniques traditionally used in spectroscopy (pressure, temperature, field or concentration jumps, photoexcitation) or physiology (electric stimulation of muscle or nerves) have also been successfully combined with X-ray scattering. Studies on magnetic orientation of biological samples are also expected to develop in the future, especially for fibrous specimens[7] as strong magnets are becoming available at several facilities.

Temperature jump and mixing experiments have been shown to be useful in the study of *in vitro* self assembly of biological macromolecules. For mixing experiments various stopped flow and continuous flow systems have been developed. The latest micromachined devices used in protein (un)folding studies, have mixing times of the order of 100 μs.[19] Temperature jumps using infrared lasers[20] or more conventional methods are also useful in time resolved studies with submillisecond resolution of phase transitions in lipids, for example. Given the importance of thermal studies for various technologies it can be expected that simultaneous recording of calorimetric and scattering data, a well-established technique, will be significantly extended by the use of micromachined devices on high brilliance sources.

Most fibre work is presently done on third generation sources with samples having diameters down to, or even below, 20 μm. Except in the case of muscle fibres, where electric stimulation can be used, perturbations are usually purely mechanical.

For grazing incidence scattering on monolayers, the amount of sample required is obviously very small but the preparative conditions are somewhat more demanding and the geometry imposes that the sample or beam be scanned to collect the entire pattern. In favourable cases like that of the membrane protein bacteriorhodopsin, which is naturally organized in a two dimensional hexagonal lattice, diffraction patterns can be obtained from a single layer deposited on an aqueous surface.[21] Multilayers can be deposited on a curved surface and their diffraction pattern including the Kiessig fringes corresponding to their thickness can be recorded without any need for scanning.[22]

At this stage many facilities are equipped with sample environments for different routine measurements, which could be partly or fully automated should the need arise.

In contrast, the possibility to image samples submitted to various kinds of perturbations seems to have been hitherto hardly exploited.

5 Detectors

The signal from solutions, non-crystalline solids or thin layers is usually much weaker than that of crystals and this puts stringent requirements on the detectors and acquisition systems. These have to cope with 3–5 orders of magnitude in intensity with a spatial resolution of 0.1–1 mm or better in the case of imaging and have typical readout times below 1 μs–10 s depending on the experiment.

The past decades have seen considerable developments in X-ray detection. On bending magnet sources most X-ray scattering measurements have been carried out with position sensitive gas detectors,[23] the use of imaging plates[24] being limited to routine static measurements. If the intensities to be measured are weak, position sensitive gas detectors, which are photon counting devices having no intrinsic noise, are still preferred by experts for accurate quantitative measurements. With instruments on insertion devices where the intensities are much higher the effect of noise in solid state detectors (*e.g.* charge coupled devices (CCD) with or without image intensifiers)[25] may become negligible. If the other distortions of these devices can be controlled they are very useful even if their slow readout prevents rapid time framing and must be replaced by less efficient procedures involving gating and synchronization with the perturbation. Pixel area detectors[26] may provide the ultimate solution for X-ray detection in the future but some development is still necessary to make them routinely usable devices.

CCD detectors can be used for imaging even though their spatial resolution is limited by the phosphors used to convert X-rays to visible light but for the most demanding applications the resolution of photographic film (5 μm) is still unbeatable.

6 Data interpretation

For a thermodynamically ideal monodisperse isotropic system like a dilute solution of proteins where the positions and orientations of the particles are uncorrelated, the scattering after appropriate scaling is simply that of a single particle averaged over all orientations, given by Debye's formula (see *e.g.*[2]):

$$I(s) = \sum_{i=1}^{N} \sum_{j=1}^{N} f_i(s) f_j(s) \frac{\sin(2\pi s r_{ij})}{2\pi s r_{ij}} \quad (2)$$

Since, as a result of spherical averaging eqn (1) is transformed into the sum of $\sin(x)/x$ terms corresponding to the distances between the N atoms in the particle in eqn (2), the intensity always decays from the origin to higher s-values. Fourier transformation yields the distance distribution of the particles, which for monodisperse particles has a value of zero beyond their largest dimension. The values of the effective scattering factors of the atoms ($f(s)$) used to calculate the scattering of particles in solution using eqn 2 depend not only on their nature but also on the electron density of the solvent. Indeed, the observable scattering results solely from the fluctuations of the electron density around that of the average value for the solvent. This also explains why one sometimes prefers to describe particles in terms of shape, contrast and internal structure (see *e.g.*[27]).

In non-ideal systems intermolecular interactions may lead to damping of the intensity near the origin, if the interactions are repulsive, or enhancement, if they are attractive. At least in the repulsive regime, the scattering of such a system can often be represented as the product of the intensity of the isolated particles and a structure factor describing the deviations from a completely random arrangement between them.

$$I(s) = I_{\text{ideal}}(s)\ S(s) \quad (3)$$

To eliminate the effect of interactions on the scattering pattern it is thus usually necessary to measure a concentration series and extrapolate to infinite dilution. As illustrated below, the interactions which may seem a nuisance in scattering measurements are put to good use in nature.

The amount of information which can legitimately be recovered from the scattering pattern of monodisperse solutions—about 10–20 independent parameters—is very limited compared to crystallography (typically 1.5×10^4 parameters for a 50 kDa protein) but still higher than for light scattering or hydrodynamic methods, which yield at best one or two independent parameters. As a consequence the temptation to overinterpret the data is never far and the questions have to be carefully chosen in order to obtain useful answers rather than just numbers.

The traditional analysis of solution scattering patterns (see *e.g.*[2]) relies on the Guinier plot ($\ln(I(s))$ *versus* s^2), which for monodisperse solutions yields a straight line. Its intercept is directly related to the molecular mass of the solute and its slope to the radius of gyration or second moment of the electron density distribution of the solute particles, which is a simple index of non-sphericity. Further interpretation depends on comparison of the experimental scattering curves with that of simple models (spheres, ellipsoids, cylinders).

About ten years ago advances in computing allowed one to turn the use of spherical harmonics for *ab initio* determination of the shape or envelope of macromolecules in solution into a practical tool.[28] Debye's formula suggested early on that models could also be built using arrangements of spheres or beads representing atoms or larger chunks of matter. This approach was often used in trial and error methods based on *a priori* information *e.g.* from electron microscopy. Bead modelling and Monte Carlo type searches have a long tradition in the interpretation of scattering patterns and a significant advance was made by systematically combining these two approaches using genetic algorithms or global searches. This led to the development of a number of software packages with different algorithms and performances in comparative tests.[29] Those developed at the EMBL (www.embl-hamburg.de/software.html) are being widely used. In the latest approach proteins are represented as an assembly of dummy residues centred at the position of the Cα atoms of the polypeptide and a chain-like structure is imposed by introducing constraints on the distribution of neighbouring dummy residues.[30] Although perhaps less general than simple bead modelling this method hitherto gives the best results for proteins and the scattering curves can be modelled up to 0.5 nm resolution.

Solutions of biological macromolecules are often polydisperse and this is obviously generally the case in time dependent phenomena like assembly processes. The information which can be extracted from the scattering patterns of such systems is, of course, more limited but singular value decomposition or least squares methods are useful in establishing the existence of intermediates depending on the available *a priori* knowledge about the species in solution.

The scattering of fibres is most naturally described in a cylindrical coordinate system and this leads to an expression similar to eqn (1) containing Bessel functions rather than familiar trigonometric functions. As real fibres are usually intermediate between the ideal non-crystalline and polycrystalline case, background subtraction is a crucial issue in data processing. Microbeams allowing one to obtain considerably better data on small oriented domains, thereby avoiding some of the averaging occurring with larger samples, are therefore extremely useful.[31] Initial models may be obtained using phases from electron microscopy or more conventional crystallographic techniques and refined using molecular dynamics or simulated annealing with suitably modified versions of crystallographic programs (for a review see[7]). An extensive collection of computer programs for data analysis which can, like the helical diffraction simulation program HELIX, also be used for educational purposes, is available through the Collaborative Computing Project in Fibre diffraction (CCP13; www.ccp13.ac.uk).

Perhaps because compared to other systems the computational effort involved in interpreting the scattering patterns of lipid phases is small there is little or no standard software for the calculation of the corresponding electron densities. For the liquid crystalline phases, the unit cell dimensions are directly obtained from the scattering patterns and the phases of the reflections can be obtained by the swelling method, for example (see *e.g*[32] and references therein). A simple method

for calculating the electron density profile of unilamellar lipid vesicles[33] and an elegant *ab initio* approach to the determination of membrane profiles[34] have recently been described.

7 Recent applications

Structural molecular biology has been largely dominated by the often implicit and somewhat dogmatic belief that all physiological function could be explained given the knowledge of static protein structures at atomic resolution. Among other techniques, static and time-resolved scattering measurements on non-crystalline systems have significantly contributed not only to correct this view, but also to highlight the importance of the properties of other components, like lipids or ions and cosolutes, for biological function.

It has become clear that crystal structures of biological macromolecules represent useful averaged snapshots of a particular conformational energy minimum but that function implies fluctuations between many conformations with not too different energies. Diffraction patterns of crystals or fibres can give some information on collective motions of atoms but this is rather well hidden in the diffuse scattering (for a review see[35]). This topic provides, however, an interesting meeting point for theory and experiment, and much progress could be made if diffuse scattering were systematically analysed as part of crystallographic data processing rather than being discarded, as is in general presently the case.

Transitions between states involving large changes in quaternary structure occur in allosteric enzymes and can easily be monitored by SAXS. The enzyme which has been most thoroughly investigated in this context is certainly aspartate transcarbamylase from *Escherichia coli* (ATCase) and it therefore provides a good measure of the current understanding of allostery. Conformational flexibility makes assemblies like ATCase particularly prone to distortions by crystal packing forces and as a result the crystal and solution structures of the catalytically active R-state differ significantly, as shown by SAXS (see[27]). This may be quite generally the case for allosteric enzymes as significant differences were also found between the structure of carbonmonoxy-hemoglobin in solution and in the crystal.[36] The extent to which the classical models of allostery—the concerted two-state Monod, Wymann, Changeux (MWC) model or the sequential Koshland, Nemethy, Filmer (KNF) model—apply in the case of ATCase is an unresolved fundamental question. Although the ultimate answer may well depend on the time resolution and sensitivity of the experiments, recent time resolved SAXS measurements using fast mixing techniques have shown that the structural transition associated with substrate binding is concerted and remains so in the presence of effectors, activators and inhibitors.[37] As illustrated in the insert in Fig. 4 the intensity of the first subsidiary maximum of the scattering pattern of ATCase is a good measure of the fraction of molecules in the T or R state. Analysis of the scattering patterns recorded during the reaction with L-aspartate and carbamyl phosphate indicates that all curves can be satisfactorily approximated as linear combinations of the reference patterns for the T- and R-states. The former is identical to the final state and the latter to the steady state. This seems to

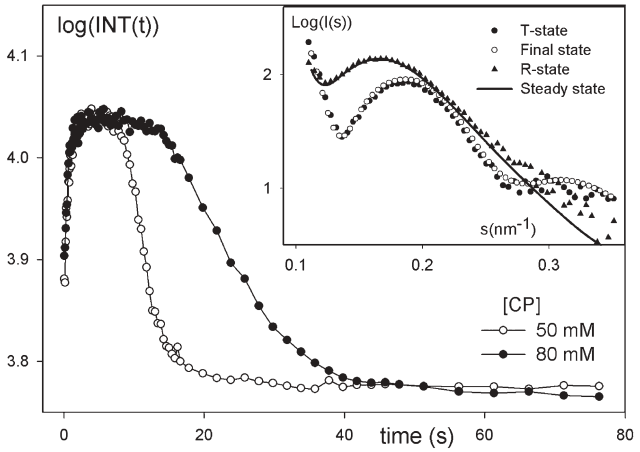

Fig. 4 Time course after stopped flow mixing of the integrated intensity in the region of the first subsidiary maximum $0.12 \leqslant s \leqslant 0.24\ \mathrm{nm}^{-1}$ for a solution of ATCase ($\sim 40\ \mathrm{mg\ ml}^{-1}$) from *E. coli* with 20% ethylene glycol at $-5\ ^{\circ}\mathrm{C}$ with [carbamyl phosphate] = [L-aspartate]. The scattering curves in the insert illustrate that the curve of the final state is identical to that of the T-state and that the steady state curve above saturating concentrations of carbamyl phosphate and aspartate is identical to that of the reference curve for the R-state (after[37]).

favour the MWC view of a concerted transition, which also predicts that inhibitors such as cytidine triphosphate (CTP) and activators such as adenosine triphosphate (ATP) act by shifting the T $\leftrightarrow$ R equilibrium. This is the case for CTP, but it is known from previous SAXS experiments that ATP alone does not affect this equilibrium. In contrast, Mg-ATP was shown to induce an even more extended conformation of the R state, as confirmed by the recent time resolved measurements.[37]

More subtle changes due to ligand-induced conformational changes can be detected in the WAXS pattern of proteins as illustrated in Fig. 5.[18] Crystallographic studies indicate that the binding of ferric ions to transferrin results in a rotation of one lobe of the protein (N1) relative to the other (N2). This domain movement results in significant changes in the small and medium angle scattering from transferrin in solution. The small sample volumes and short exposure times required for such measurements suggest that this technique could be used for *in vitro* ligand screening.

These two examples clearly illustrates the complementarity of the SAXS and high resolution crystallographic approaches in the investigation of structural transitions of complex systems.

Other transitions accompanied by large structural changes are those associated with the (un)folding of proteins or nucleic acids. Shape determination may still be useful to characterize the early stages of unfolding as illustrated in Fig. 6 for the reversible thermal denaturation of lysozyme, a process that has been investigated in detail by different biophysical techniques. The increase of the slope of the scattering curve betrays the partial unfolding which does not proceed further as long as the four disulfide bridges in the molecule remain intact. Complete unfolding would lead to a scattering pattern corresponding to a statistical chain with persistence or Kratky–Porod chain (see *e.g.*[27]).

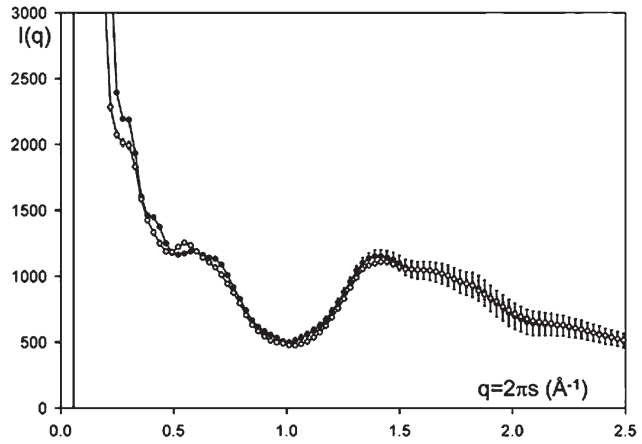

Fig. 5 WAXS pattern of apotransferrin (•) and transferrin with Fe^{3+} bound (40 mg ml^{-1} in 25 mM Tris-HCl pH 8.0) recorded in seven independent 5 s frames using a CCD detector on beamline 18ID at the APS, Argonne. The irradiated sample volume was ~20 μl per frame. The difference due to the relative rotation of the N1 and N2 lobes of the protein upon iron binding mainly affects the intensity in the low and medium angle region.[18]

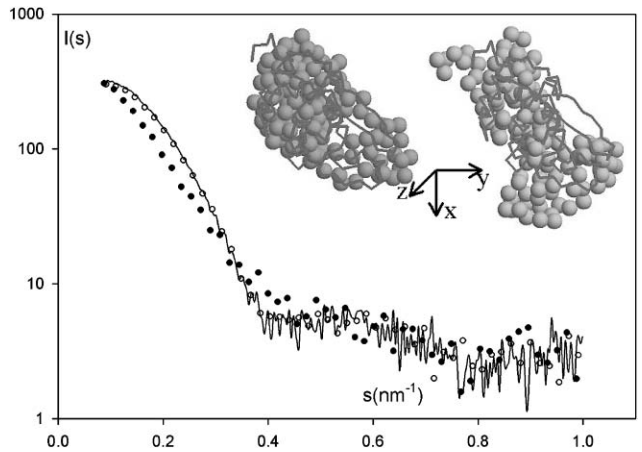

Fig. 6 Scattering patterns of a lysozyme solution (37 mg ml^{-1} in 40 mM Na-acetate) at 80 °C (●) and at 20 °C before (—) and after (○) heating. The models in the insert were calculated from the scattering curve using the program GASBOR.[30] They are superimposed on the trace of the chain obtained from the crystal structure to illustrate the reversible partial unfolding of lysozyme upon heating. (Courtesy of W. Shang.)

Time resolved scattering patterns recorded during (un)folding processes, where the key steps occur in the μs–ms range, allow one to characterize average dimensions of intermediate states but their detailed interpretation usually requires parallel spectroscopic measurements (*e.g.* circular dichroism and fluorescence).[38] These studies are important because they provide crucial experimental tests for current theories of protein folding. RNA folding occurs over a similar time range but with mechanisms that differ from those of protein folding particularly because electrostatic rather than hydrophobic interactions dominate the process (see[27]).

For *in vitro* assembly studies of viruses or components of the cytoskeleton like microtubules, SAXS and cryoelectron microscopy are indispensable complementary tools, as clearly illustrated in a recent study of the maturation of *Nudaurella capensis* omega virus.[39] This is an area where much remains to be done also in connection with applications in nanotechnology.

Further examples of applications of SAXS to the study of proteins, nucleic acids and their complexes can be found in recent reviews (*e.g.*[40,27]).

Although the aim of most present SAXS studies on biological macromolecules is to model their shape or that of their complexes in solution and/or detect large conformational changes, the technique is also well suited for studying intermolecular interactions in solutions. Protein interactions at high concentrations play a crucial role in physiological processes like vision, for example. Indeed, although the eye lens has one of the highest concentrations of proteins (crystallins) in the body, the strong intermolecular repulsions lead to liquid-like short range order which prevents light scattering. Association of the crystallins with age or due to diseases like diabetes disrupts this short range order and leads to increased scattering and cataract. The contribution of extensive SAXS studies, which have clarified the role of the different types of crystallins (α,β,γ) in the transparency of the lens, have been recently reviewed in the context of other structural and biochemical investigations.[41] Another example is that of marine animals and organs like kidneys where the stability of proteins and their interactions are regulated by large concentrations of osmolytes like urea or trimethylamine-*N*-oxide. The effects of such substances, which mainly affect the properties of water, on the interactions between proteins in concentrated solutions can easily be detected by SAXS.[42]

The two examples above illustrate that the focus on atomic structures of macromolecules, which has taken much of the attention away from the crucial effects of ions or cosolutes on the solution behaviour of DNA, proteins or charged polysaccharides like the carrageenans or hyaluronic acid, also has created some blind spots. As pointed out by the late David Blow in his introduction to a recent biophysics textbook,[43] "As understanding of biological processes extends towards modelling them by strict physical rules, the weakness of this area of biophysical analysis becomes more embarrassingly apparent". Anomalous SAXS (ASAXS) may help remedying this situation as it is one of the few techniques which may provide a window on the distribution of counterions around polyelectrolytes. Although these experiments and their interpretation are not straightforward, the few detailed studies available have already provided unique data for testing current theories on counterion condensation[44] or like-charge attractions in polyelectrolytes.[45] Beside their theoretical importance such studies are often also of direct practical relevance as properties like salt induced gelation make polysaccharides important substances in the food industry and in pharmaceutical technology.

Structural studies of lipid assemblies raise entirely different questions than those on proteins or nucleic acids. Lipids are unique in that they combine two quite independent structural levels, one with long range order, the other with short range (dis)order. At low temperatures or in pure lipid systems the chains can be well ordered but this is generally not the case in physiological conditions. The short range disorder, or fluidity

of the chains, can easily be characterized by Fourier transform infrared spectroscopy, whereas the long range order is best monitored by X-ray scattering. Although the structural phase diagrams of lipid systems have been extensively investigated during the last decades these studies remain important. Indeed, although the structure that is considered biologically most relevant is that of the bilayers associated with the L_α phase,[46] there is growing evidence that the polymorphism of lipids and in particular their ability to form cubic phases play a role in several important physiological processes.[8] The potential of lipid A from Gram-negative bacteria to cause sepsis has, for example, been correlated with their tendency to form cubic phases.[47] Cubic phases also offer an attractive crystallisation medium for membrane proteins and a recent survey indicates that about 15% of the known structures of membrane proteins were determined using crystals obtained by this method.[48]

Two particularly interesting results were recently obtained in the membrane field. The first one was the direct characterization of a membrane fusion intermediate structure, a so-called stalk, by X-ray diffraction.[49] The second, perhaps even more spectacular, was the observation of subtle changes in the structure of the axonal membrane of the unmyelinated pike olfactory nerve indicating that chemical depolarization is accompanied by an increase in thickness of the membrane.[34] This effect as well as that of some drugs and local anaesthetics, which also affect membrane thickness, can be interpreted in terms of a modulation of the conformational disorder of the hydrocarbon chains of the lipid molecules. This group is now also investigating the time course of these processes at the ESRF.

The extensive polymorphism of lipids and lipid–protein or lipid–nucleic acids systems suggests that they may have practical applications as drug or even gene delivery systems (see *e.g.*[50]). The monoolein–water system is one of those being investigated in this context because in the fully hydrated state it forms a cubic phase consisting of a three dimensional network separating two identical water channel systems with a pore diameter of about 5 nm. Such a structure may accommodate hydro-, amphi- or lipophilic molecules in its regions of different polarity.

As illustrated in Fig. 7 for an aqueous dispersion of monoolein, the properties of such systems depend very much on their preparative conditions, and time resolved X-ray scattering is one of the key methods for monitoring the changes during processing.

Today most applications of fibre diffraction are in the realm of synthetic polymers and composite or hierarchical materials like wood or bone. With third generation SR sources, experiments on single muscle fibres[51] or even on live Drosophila[52] can now be done with sub-millisecond time resolution. For such systems the development of microfocus cameras[31] has opened new possibilities of correlating the structure at the nm–μm scale with macroscopic mechanical properties.

This is important because many properties of materials depend on their arrangement on the nm–μm scale rather than

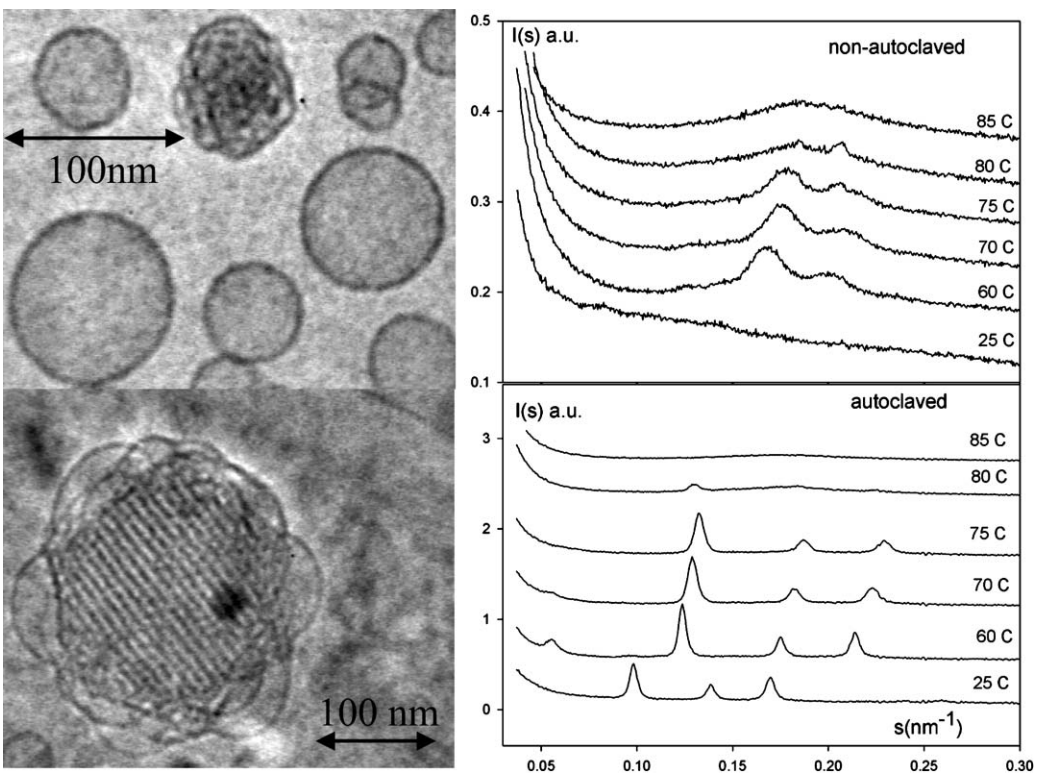

Fig. 7 Electron micrographs of aqueous dispersions of monoolein (M) and poloxamer (P) with P/(M + P) = 0.12, indicate that non-autoclaved dispersions (top, left) contain essentially unstructured vesicles (~90 nm ø) and a small number of particles with a structured interior. In contrast, the particles in the autoclaved dispersions (bottom, left) are significantly larger (~300 nm ø) and the corresponding SAXS pattern (bottom, right) clearly reveals their cubic internal structure. Although the dimensions of the structure change as indicated by the shift of the reflections with increasing temperature it is maintained well above physiological temperatures. The exact mechanism of the transition is still unknown but seems to require the formation of a transient isotropic phase. (For details see.[57])

at the atomic level and biological systems and biopolymers are no exception. Solid polysaccharides like starch, cellulose or inulin form semi-crystalline systems consisting of stacks of periodically alternating amorphous and crystalline regions similar to those found in many synthetic polymers. As illustrated in Fig. 8, this gives rise to a characteristic side maximum in the SAXS pattern corresponding to the periodicity of the different regions which can easily be monitored during the treatments typically used in food processing. The degree of crystallinity which can be extracted from the corresponding linear correlation function or from the intensity of the wide angle scattering pattern can be related to daily phenomena like the staling of bread or the organoleptic properties of rice, for example. Although X-ray data are usually recorded on bulk material the mechanisms of processes like hydration can be studied *in situ* on isolated grains using microfocus cameras.[31] Combined with optical microscopy these instruments are particularly useful in the study of hierarchical materials like wood and bone.

The excellent mechanical properties of wood are among others related to the orientation of the cellulose fibrils which are embedded in a matrix of hemicelluloses and lignin. Scanning microdiffraction revealed that these fibrils form a helix around the cells as illustrated in Fig. 9. By combining tensile tests and microdiffraction on individual wood cells and on wood foils it could be shown that recovery after deformation relies mainly on a stick–slip mechanism, which reforms the amorphous matrix between the cellulose microfibrils within the cell wall and yields a plastic response similar to that of dislocations in metals.[53] Such results not only help understand biomechanics, but also give useful hints for the development of new synthetic materials.

When the structures become sufficiently large the coherence properties of third generation sources offer unique possibilities

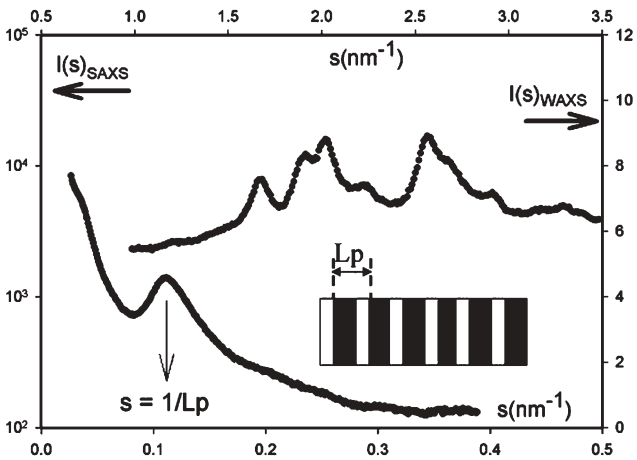

Fig. 8 SAXS pattern of milled rice flour (puntal, apparent amylose content 24%, moisture content 66%). The semi-crystalline structure with alternating crystalline and amorphous regions which has a repeat, or long period, Lp as shown in the insert, gives rise to a characteristic side maximum at an *s*-value corresponding to the inverse of the long period. The WAXS pattern is due to diffraction from the crystalline regions. (Courtesy of Veerle Derycke, Laboratory of Food Chemistry, Katholieke Universiteit Leuven.)

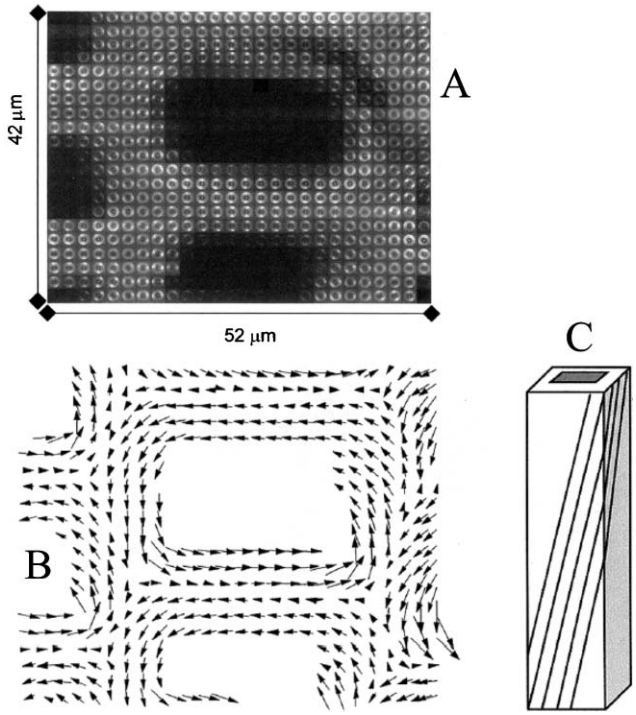

Fig. 9 Mesh scan with a 2 × 2 μm^2 X-ray beam over a complete wood cell and parts of the neighbouring cells in the S2 layer of wood of Norwegian spruce (*Picea abies*) (A). Dark regions correspond to lumina, bright ones to cell walls. Each circular sub-image is a diffraction pattern from which the local orientation of the cellulose fibrils in the slice can be deduced as indicated in the corresponding arrow map (B). By combining the results for several slices a three dimensional model of the right-handed Z-helix traced around the cell by the cellulose fibrils is obtained (C) (After,[58] ©IUCr, with permission.)

for direct imaging and the penetration depth of X-rays makes microtomography an attractive possibility.

Although such methods still need to be fully developed there is already no doubt that they can contribute to answer important questions in physiology. The best example is provided by a recent phase contrast imaging study which has uncovered a new respiratory mechanism in land insects.[54] By making videos of living breathing insects with 16.7 ms time resolution (60 Hz) using 25 keV synchrotron X-rays, rapid cycles (<1 s) of tracheal compression and expansion could be observed in the head and thorax as illustrated in Fig. 10. This previously unknown mechanism, which complements those of gas diffusion, hemolymph movement and autoventilation, has some analogy with the inflation–deflation mechanism of vertebrate lungs. Whether the same mechanism is used in the closed tracheal system of aquatic insects which also have to cope with hydrostatic pressure remains, however, an open question.

8 Conclusions and future prospects

The examples above which are based on developments in various aspects—instrumentation, experimental techniques and software—of scattering and related imaging methods during the last decades clearly demonstrate the ability of these

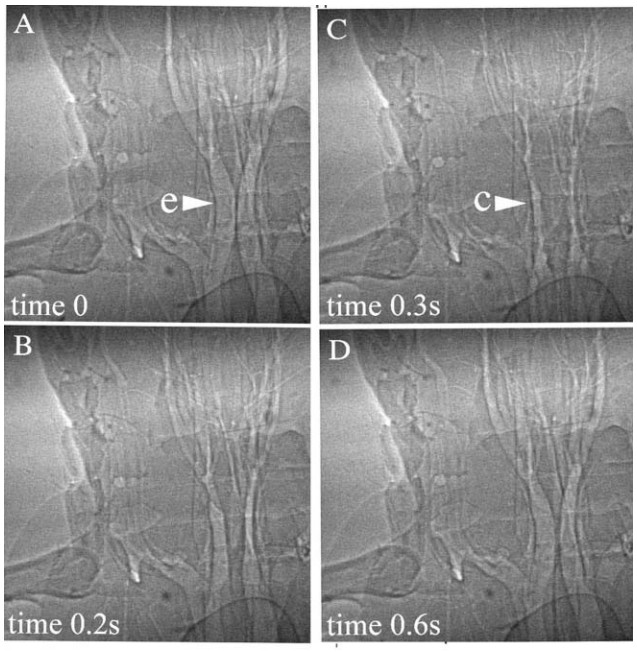

Fig. 10 Dorsoventral views (head up, posterior part bottom) of the head and thorax of the beetle *Platynus decentis* at 0.3 s intervals during a respiratory cycle of tracheal compression. At rest (A) the tracheal tubes are expanded (arrowhead e). Lateral compression occurs throughout the anterior region of the insect and results in narrowing of the tracheae in dorsal view and their expansion in lateral view (not shown). Maximal compression (C, arrowhead c) is rapidly followed by expansion of the tracheae (D). (After,[54] ©AAAS, with permission.)

techniques to contribute to the solution of problems relevant to the life sciences and materials science.

The most challenging problems—fundamental and applied—are, certainly for chemists, not only related to the description of structures but to the understanding and ultimately the control of the structural changes accompanying the functioning of biological systems or the processing of materials. All, even modest, progress in this direction, should be welcomed and scattering and imaging methods are an important tool in this endeavour. Several excellent SR sources are available in the USA such as the Advanced Photon Source (APS www.aps.anl.gov) or the Stanford Synchrotron Radiation Laboratory (SSRL www.ssrl.slac.stanford.edu) and Japan (SPring 8 www.spring8.or.jp/e/). In principle, scientists in Europe are also well equipped as most second generation machines will be phased out during the next decade and replaced by new third generation sources: (ESRF www.esrf.fr), Swiss Light source, SLS, (sls.web.psi.ch), Diamond (www.diamond.ac.uk), Soleil (www.synchrotron-soleil.fr) and PETRA III (petra3.desy.de). ESRF, SLS, Diamond and the APS have the additional advantage of being located in the vicinity of neutron sources, which should facilitate complementary experiments.

There is undoubtedly still considerable potential for developments in X-ray scattering and imaging techniques and their applications. Some of the most fascinating questions are those related to the use of the coherence properties of high brilliance sources for imaging[12] and of short pulses for the study of chemical reactions[55] or phase transitions[56] using X-ray scattering. Somewhat further into the future the fourth generation sources, X-ray free electron lasers (XFEL) with their extremely high brilliance, coherence and short pulses represent paradoxically the kind of leap in the dark which occasionally provides entirely unexpected science and technology. The construction of a reliable XFEL is at this stage certainly the most challenging project for machine physicists, but alternative ways of producing X-rays with desirable properties such as coherence or short pulses (*e.g.* using lasers beams) are certainly also worth investigating.

The driving force of individual scientists and indispensable binding element between the members of any successful team, who have to master an increasingly wider range of skills, will always remain to be contributing to finding answers to the legitimate questions, which they should ideally be able to choose freely. Therefore, the major challenge for large facilities, if they want to remain successful, will be to provide, also in the future, a sufficient number of niches where such exploratory behaviour is possible and new methods can be developed, while continuing to provide access and support to experts in other fields.

Acknowledgements

The author thanks H. Bunjes, V. Derycke, R. Fischetti, P. Fratzl, S. Funari, B. Lengeler, L. Makowski, M. Rappolt, C. Riekel, W. Shang, A. Snigirev, H. Tsuruta, P. Vachette, M. Westneat, G. Wörle for the many helpful suggestions and the material they provided for the preparation of this review.

References

1 J. S. Pedersen, *J. Appl. Crystallogr.*, 2004, **37**, 369.
2 C. Cantor and P. Schimmel, *Biophysical Chemistry: II Techniques for the study of biological structure and function*, W. H. Freeman & Co., New York, New York, USA, 1980.
3 A. Guinier, *Ann. Phys. (Paris)*, 1939, **12**, 161.
4 H. B. Stuhrmann and A. Miller, *J. Appl. Crystallogr.*, 1978, **11**, 325.
5 G. Rosenbaum, K. C. Holmes and J. Witz, *Nature*, 1971, **230**, 434.
6 W. Cochran, F. H. C. Crick and V. Vand, *Acta Crystallogr.*, 1952, **5**, 581.
7 G. Stubbs, *Curr. Opin. Struct. Biol.*, 1999, **9**, 615.
8 V. Luzzati, *Curr. Opin. Struct. Biol.*, 1997, **7**, 661.
9 J. Als-Nielsen, D. Jacquemain, K. Kjaer, F. Leveiller, M. Lahav and L. Leiserowitz, *Phys. Rep.*, 1994, **246**, 251.
10 C. G. Schroer, P. Cloetens, M. Rivers, A. Snigirev, A. Takeuchi and W. B. Yun, *MRS Bull.*, 2004, **29**, 157.
11 C. G. Schroer and B. Lengeler, *Phys. Rev. Lett.*, 2005, **94**, 054801.
12 J. W. Miao, H. N. Chapman, J. Kirz, D. Sayre and K. O. Hodgson, *Annu. Rev. Biophys. Biomol. Struct.*, 2004, **33**, 157.
13 A. Snigirev, I. Snigireva, V. Kohn, S. Kuznetsov and I. Schelokov, *Rev. Sci. Instrum.*, 1995, **66**, 5486.
14 N. J. Terrill, A. F. Grant, A. R. Marshall, A. D. Smith and K. J. Sawhney, *Fibre Diffract. Rev.*, 2004, **12**, 9.
15 B. Lengeler, *Naturwissenschaften*, 2001, **88**, 249.
16 L. E. Levine and G. G. Long, *J. Appl. Crystallogr.*, 2004, **37**, 757.
17 J. Bordas, G. R. Mant, G. P. Diakun and C. Nave, *J. Cell Biol.*, 1987, **105**, 1311.
18 R. F. Fischetti, D. J. Rodi, D. B. Gore and L. Makowski, *Chem. Biol.*, 2004, **11**, 1.
19 S. Akiyama, S. Takahashi, T. Kimura, K. Ishimori, I. Morishima, Y. Nishikawa and T. Fujisawa, *Proc. Natl. Acad. Sci. USA*, 2002, **99**, 1329.
20 M. Kriechbaum, G. Rapp, J. Hendrix and P. Laggner, *Rev. Sci. Instrum.*, 1989, **60**, 2541.

21 S. A. W. Verclas, P. B. Howes, K. Kjaer, A. Wurlitzer, M. Weygand, G. Buldt, N. A. Dencher and M. Losche, *J. Mol. Biol.*, 1999, **287**, 837.
22 G. Rapp, M. H. J. Koch, U. Hoehne, Y. Lvov and H. Moehwald, *Langmuir*, 1995, **11**, 2348.
23 A.-M. Petrascu, M. H. J. Koch and A. Gabriel, *J. Macromol. Sci., Physics*, 1998, **B37**, 463.
24 Y. Amemiya, *Methods Enzymol.*, 1997, **276**, 233.
25 V. Urban, P. Panine, C. Ponchut, P. Boesecke and T. Narayanan, *J. Appl. Crystallogr.*, 2003, **36**, 809.
26 B. Schmitt, C. Bronnimann, E. F. Eikenberry, G. Hulsen, H. Toyokawa, R. Horisberger, F. Gozzo, B. Patterson, C. Schulze-Briese and T. Tomizaki, *Nuclear Instrum. Methods*, 2004, **A518**, 436.
27 M. H. J. Koch, P. Vachette and D. I. Svergun, *Q. Rev. Biophys.*, 2003, **36**, 147.
28 D. I. Svergun, V. V. Volkov, M. B. Kozin, H. B. Stuhrmann, C. Barberato and M. H. J. Koch, *J. Appl. Crystallogr.*, 1997, **30**, 798.
29 P. Zipper and H. Durchschlag, *J. Appl. Crystallogr.*, 2003, **36**, 509.
30 D. I. Svergun, M. V. Petoukhov and M. H. J. Koch, *Biophys. J.*, 2001, **80**, 2946.
31 C. Riekel, *Rep. Prog. Phys.*, 2000, **63**, 233.
32 M. Rappolt, A. Hickel, F. Bringezu and K. Lohner, *Biophys. J.*, 2003, **84**, 3111.
33 M. R. Brzutowicz and A. T. Brunger, *J. Appl. Crystallogr.*, 2005, **38**, 126.
34 V. Luzzati, P. Vachette, E. Benoit and G. Charpentier, *J. Mol. Biol.*, 2004, **343**, 187.
35 J. B. Clarage and G. N. Phillips, Jr., *Methods Enzymol.*, 1997, **277**, 407.
36 J. A. Lukin, G. Kontaxis, V. Simplaceanu, Y. Yuan, A. Bax and C. Ho, *Proc. Natl. Acad. Sci. USA*, 2003, **100**, 517.
37 H. Tsuruta, H. Kihara, T. Sano, Y. Amemiya and P. Vachette, *J. Mol. Biol.*, 2005, **348**, 195.
38 T. Kimura, T. Uzawa, K. Ishimori, I. Morishima, S. Takahashi, T. Konno, S. Akiyama and T. Fujisawa, *Proc. Natl. Acad. Sci. USA*, 2005, **102**, 2748.
39 M. A. Canady, H. Tsuruta and J. E. Johnson, *J. Mol. Biol.*, 2001, **311**, 803.
40 S. Doniach, *Chem. Rev.*, 2001, **101**, 1763.
41 H. Bloemendal, W. de Jong, R. Jaenicke, N. H. Lubsen, C. Slingsby and A. Tardieu, *Prog. Biophys. Mol. Biol.*, 2004, **86**, 407.
42 M. Niebuhr and M. H. J. Koch, *Biophys. J.*, 2005, **89**, 1978.
43 M. Daune, *Molecular Biophysics*, Oxford University Press, Oxford, UK, 1999.
44 Y. Bai, R. Das, I. S. Millett, D. Herschlag and S. Doniach, *Proc. Natl. Acad. Sci. USA*, 2005, **102**, 1035.
45 T. E. Angelini, H. Liang, W. Wriggers and G. C. L. Wong, *Proc. Natl. Acad. Sci. USA*, 2003, **100**, 8634.
46 M. Rappolt, P. Laggner and G. Pabst, *Recent Res. Dev. Biophys.*, 2004, **3**, 363.
47 U. Seydel, L. Hawkins, A. Schromm, H. Heine, O. Scheel, M. H. J. Koch and K. Brandenburg, *Eur. J. Immunol.*, 2003, **33**, 1586.
48 L. V. Misquitta, Y. Misquitta, V. Cherezov, O. Slattery, J. M. Moham, D. Hart, M. Zhalnina, W. A. Cramer and M. Caffrey, *Structure*, 2004, **12**, 2113.
49 L. Yang and H. W. Huang, *Science*, 2002, **297**, 1877.
50 D. Mirska, K. Schirmer, S. S. Funari, A. Langner, B. Dobner and G. Brezesinski, *Colloids Surf., B*, 2004, **40**, 51.
51 M. Reconditi, M. Linari, L. Lucii, A. Stewart, Y.-B. Sun, P. Boesecke, T. Narayanan, R. F. Fischetti, T. Irving, G. Piazzesi, M. Irving and V. Lombardi, *Nature*, 2004, **428**, 578.
52 M. Dickinson, G. Farman, M. Frye, T. Bekyarova, D. Gore, D. Maugham and T. Irving, *Nature*, 2005, **433**, 330.
53 J. Keckes, I. Burgert, K. Fruehmann, M. Mueller, K. Koelln, M. Hamilton, M. Burghammer, S. V. Roth, S. Stanzl-Tschegg and P. Fratzl, *Nat. Mater.*, 2003, **2**, 810.
54 M. W. Westneat, O. Betz, R. W. Blob, K. Fezzaa, W. J. Cooper and W.-K. Lee, *Science*, 2003, **299**, 558.
55 H. Ihee, M. Lorenc, T. K. Kim, Q. Y. Kong, M. Cammarata, J. H. Lee, S. Bratos and M. Wulff, *Science*, 2005, **309**, 1223.
56 A. M. Lindenberg, J. Larsson, K. Sokolowski-Tinten, K. J. Gaffney, C. Blome, O. Synnergren, J. Sheppard, C. Caleman, A. G. MacPhee, D. Weinstein, D. P. Lowney, T. K. Allison, T. Matthews, R. W. Falcone, A. L. Cavalieri, D. M. Fritz, S. H. Lee, P. H. Bucksbaum, D. A. Reis, J. Rudati, P. H. Fuoss, C. C. Kao, D. P. Siddons, R. Pahl, J. Als-Nielsen, S. Duesterer, R. Ischebeck, H. Schlarb, H. Schulte-Schrepping, T. Tschentscher, J. Schneider, D. von der Linde, O. Hignette, F. Sette, H. N. Chapman, R. W. Lee, T. N. Hansen, S. Techert, J. S. Wark, M. Bergh, G. Huldt, D. van der Spoel, N. Timneanu, J. Hajdu, R. A. Akre, E. Bong, P. Krejcik, J. Arthur, S. Brennan, K. Luening and J. B. Hastings, *Science*, 2005, **308**, 392.
57 G. Wörle, B. Siekmann, M. H. J. Koch and H. Bunjes, *Eur. J. Pharm. Sci.*, 2005.
58 H. Lichtenegger, M. Muller, O. Paris, C. Riekel and P. Fratzl, *J. Appl. Crystallogr.*, 1999, **32**, 1127.